Photoreactions in polymers containing benzil units: a comparative study under excimer laser and Hg-lamp irradiation

H. Simbürger[a], W. Kern[a,*], K. Hummel[a], C. Hagg[b]

[a]*Institut für Chemische Technologie organischer Stoffe, Technische Universität, Graz, Stremayrgasse 16, A-8010 Graz, Austria*
[b]*Institut für Chemische Technologie anorganischer Stoffe, Technische Universität, Graz, Stremayrgasse 16, A-8010 Graz, Austria*

Abstract

Polymers bearing benzil units in the main chain (polymer I, poly(oxyhexyleneoxy-4,4′-benzilylene) and polymer II, poly(oxy-4,4′-benzilyleneoxysebacoyl) or as pendant side groups (polymer III, poly(phenyl methacrylate)-*co*-4-methacryloyloxy-4′-methoxybenzil) were synthesized via polycondensation and free radical polymerization. The polymers became crosslinked during u.v. irradiation and were assessed as potential negative resist materials. The lithographic sensitivity (i.e. the onset of gel formation) of *polymers I–III* depended on the irradiation source (Hg-lamp, 311 nm; excimer laser, 308 nm) and on the pulse energy of the excimer laser (50–400 J m^{-2}). For example, for polymer I the onset of gel formation dropped from $E'_g = 2000$ J m^{-2} to $E'_g = 400$ J m^{-2} when the laser pulse energy was raised from 100 to 400 J m^{-2}. The sensitivity under continuous Hg-lamp irradiation was similar to that under low-energy laser irradiation. A Charlesby–Pinner analysis of the crosslinking data revealed that both crosslinking and chain fragmentation occurred during u.v. irradiation $(0.24 < \Phi_{CS} \cdot \Phi_{CL}^{-1} < 0.54)$. During u.v. irradiation, the benzil chromophores and—in the case of polymer II—also the ester units were transformed during u.v. irradiation. FT i.r. data showed that the photoreactions and their efficiency varied depending on the excitation source. These laser-specific reactions are probably due to two-photon processes. © 2000 Elsevier Science Ltd. All rights reserved.

Keywords: Photoreactive polymer; Benzil; Excimer laser

1. Introduction

The photochemistry of benzil has been the subject of several studies [1–13]. Under Hg-lamp irradiation, benzil is excited to its singlet state S_1 and the triplet state T_1 is then formed via intersystem crossing (ISC). Hydrogen abstraction from donor molecules leads to the formation of the benzil ketyl radical (see Scheme 1; photoreaction of benzil under Hg-lamp irradiation (311 nm)). When benzil is irradiated in the presence of amines, an exciplex is formed which is further deactivated to an aminyl radical and the benzil ketyl radical [4].

Other investigations were concerned with the photoreactions of benzil in the presence of oxygen. Lukác and Kósa [12] reported the formation of dibenzoylperoxide as an intermediate, which gives rise to the formation of various photoproducts under Hg-lamp irradiation. In addition, benzil has been examined as a photoinitiator for the polymerization of acrylic monomers [14].

When solutions of benzil are irradiated with the pulsed light from an excimer laser (308 nm), a homolytic fragmentation into benzoyl radicals occurs. This has been investigated by transient u.v. spectroscopy [6], ESR spectroscopy [15] and time-resolved EPR (TREPR) studies [9]. Generally, this photoreaction is not observed under continuous Hg-lamp irradiation.

McGimpsey and Scaiano [6,7] carried out a close investigation of the two-photon photochemistry of benzil. Solutions of benzil were irradiated with an excimer laser pulse (308 nm) and a subsequent dye laser pulse (517 nm; 0.75 μs delay). It was shown that benzil triplets (T_1; produced by the first laser pulse) decay when irradiated with the second laser pulse. Furthermore it was shown that a two-photon absorption also occurs during irradiation with 308 nm laser pulses only. The authors concluded that benzil triplets (T_1) compete for absorption towards the end of the 308 nm laser pulse, since the absorption coefficient ε_{308} of the triplet state T_1 is four times larger than ε_{308} of ground state benzil. The absorption of a second photon then leads to the homolytic cleavage of benzil into benzoyl radicals [6,7].

On the other hand, Mukai and Yamauchi [9] reported that benzil is initially excited to the S_1 state by absorption of the

* Corresponding author. Tel.: + 43-316-873-8957; fax: + 43-316-873-8951.
E-mail address: kern@ictos.tu-graz.ac.at (W. Kern).

Scheme 1.
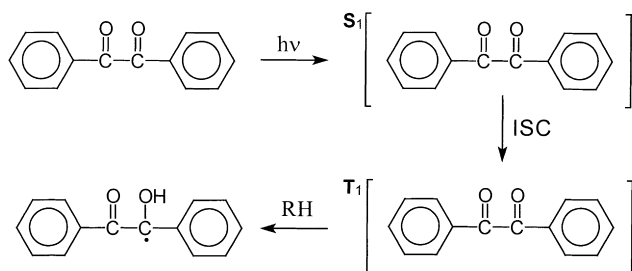
first photon. Subsequent absorption of a second photon generates a higher singlet state S_n, which is then converted to the triplet state T_n by ISC. Benzoyl radicals are then formed by the dissociation of the T_n state of benzil. Mukai and Yamauchi stated that direct $T_1 \rightarrow T_n$ excitation does not occur. This was concluded from TREPR experiments, which showed an inversion of the polarization of the emissive signal as a result of $S_1 \rightarrow S_n$ excitation followed by $S_n \rightarrow T_n$ ISC. The photoreactions of benzil under excimer laser irradiation are summarized in Scheme 2 (photoreactions of benzil under excimer laser irradiation (308 nm)).

Although much work has been devoted to the photoreactions of benzil and its derivatives, only a few reports deal with the photochemistry of polymers bearing benzil units. As an example, Lukác et al. prepared polymers with benzil units in the side chain and investigated their fluorescence spectra [16] as well as their photoreactions [17] under Hg-lamp illumination. To date, such polymers have not

been investigated under laser irradiation with regard to the possibility of two-photon reactions.

The aim of the present investigation was a photochemical study of polymers containing benzil units in the main chain or as pendant side groups. The photochemical yields of crosslinking and chain fragmentation in polymers of this kind were examined both under Hg-lamp and under excimer laser irradiation. As explained above, the photochemistry of benzil depends on the irradiation source. We wished to see if the photoprocesses in these polymers also vary depending on the type of illumination.

It is expected that excimer lasers will be the workhorse of the future in microlithography [18] since excimer lasers provide high-intensity monochromatic radiation in the deep u.v. range, where Hg-lamps emit only low intensities. Over the past years, numerous resist materials for laser exposure have been presented, but only in a few cases the sensitivity was found to be different under Hg-lamp and laser irradiation (e.g. see Ref. [19]). In this connection, the present paper is a contribution towards the development of new photoresist materials for excimer laser processing.

2. Experimental

Lamp irradiations were carried out with a 1300 W mercury lamp (Heraeus Q 1023) equipped with a 311 nm interference filter (Melles Griot, type 03FIM024). The light intensity at the sample surface was determined by ferrioxalate actinometry
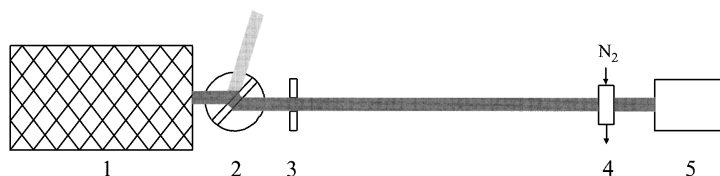

Scheme 2.
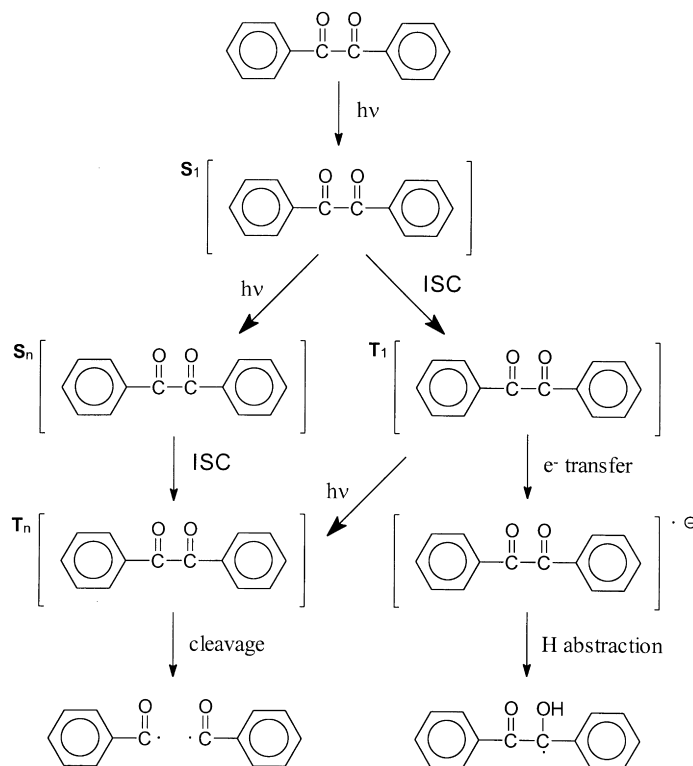
Fig. 1. Experimental setup for excimer laser irradiation: (1) laser; (2) dielectric attenuator plate; (3) beam shaper; (4) irradiation chamber; and (5) pyroelectric detector.

[20]. For irradiation with pulsed u.v. light, an excimer laser (Lambda Physik LPX 105 i) was applied (XeCl, 308 nm, 20 ns pulse duration, repetition rate 1 Hz). The beam was homogenized with a beam shaper (Optec, type HY120) and attenuated with dielectric attenuator plates (Optec, type AT4030). The pulse energy was monitored with a pyroelectric detector (Gentec ED200). The light path is sketched in Fig. 1. Fig. 2 shows the sample holder used for the irradiation of the polymer films under inert gas atmosphere. Solutions were irradiated in quartz cuvettes (pathlength 0.5 mm). Prior to and during irradiation, a stream of nitrogen was passed through the solutions to exclude oxygen.

2.1. Analytical instrumentation

Gas chromatography (GC) was performed with a Hewlett Packard HP 6890 gas chromatograph (HP 5 silicon column, FID detector). Infrared (FT i.r.) spectra were recorded with a Bomem Michelson 100 FT i.r. spectrometer, u.v. spectra were taken with a Hewlett Packard HP8452A diode array spectrometer. ^{1}H n.m.r. spectra were recorded with a Bruker MSL 200 n.m.r. spectrometer. DSC runs and thermogravimetry were performed with a thermal analyser from Polymer Laboratories (model STA 625).

The average molecular weight (M_w) and the polydispersity index PDI $= M_w \cdot M_n^{-1}$ were determined by size exclusion chromatography (SEC) with polystyrene–divinylbenzene gel columns (10^3, 10^4 and 10^5 Å, particle size 5 μm, from Polymer Standard Services, eluent tetrahydrofuran) using a Viscotec Model 200 differential refractometer/viscometer as detector. The calibration was carried out with polystyrene standards (obtained from Polymer Standards Services).

2.2. Photocrosslinking experiments

Sol–gel data (sensitometric curves) were obtained by the following procedure: polymer films were spincast onto CaF$_2$ plates from chloroform solutions (10–15 kg m^{-3}). Spincasting was performed with a Suss RC 5 spin coater. After drying for at least 4 h in vacuo, the films were irradiated under nitrogen atmosphere. The irradiated films were developed by immersion in dichloromethane (30 min at 20°C) and then dried again in vacuo. Before and after development, absorbance FT i.r. spectra were taken. The soluble fraction *S* was calculated from the FT i.r. absorbance of appropriate peaks, which remained unchanged during irradiation.

Absolute film thicknesses were obtained by section analysis with an atomic force microscope (AFM) in the tapping mode (Nanoscope 3 from Digital Instruments, Santa Barbara, USA). Using a needle, a groove was gently scratched into the polymer film in order to minimize damage of the substrate. The tip of the atomic force microscope was moved at right angle across the groove to give a height profile. The absolute film thickness measured was then related to absorbance data obtained from FT i.r. spectra. The thickness of the polymer films investigated ranged between 200 and 500 nm. In all cases, the u.v. absorbance at 308 (311) nm was kept below 0.4 to ensure an uniform illumination of the polymer films throughout their depth.

The structures of polymers I–III are shown in Scheme 3 (structures of polymers I–III).

2.2.1. Synthesis of 4,4′-dihydroxybenzil (DHB)

4,4′-Dimethoxybenzil (20.0 g, 74 mmol) and well dried pyridinium hydrochloride (44.0 g, 381 mmol) were mixed and then heated at 180°C under exclusion of moisture (5 h). The crude product was purified by two-fold column chromatography (silica gel 60) using cyclohexane/ethyl acetate (vol. ratio 10:8) as eluent. Yield of 4,4′-dihydroxybenzil: 75% (13.6 g, 56 mmol). M.p. 250–251°C. FT i.r. data (KBr pellet) are compiled in Table 1, ^{1}H n.m.r. data (CDCl$_3$) are given in Table 2.

2.2.2. Synthesis of 4-hydroxy-4′-methoxybenzil (HMB)

4,4′-Dimethoxybenzil (20.0 g, 74 mmol) and well-dried pyridinium hydrochloride (44.0 g, 381 mmol) were mixed and then heated at 180°C for approximately 120 min. Every 15 min, the conversion was controlled by thin layer chromatography in order to prevent excessive formation of 4,4′-dihydroxybenzil. Under these reaction conditions, 4-hydroxy-4′-methoxybenzil was obtained in addition to 4,4′-dihydroxybenzil. After column chromatography (silica
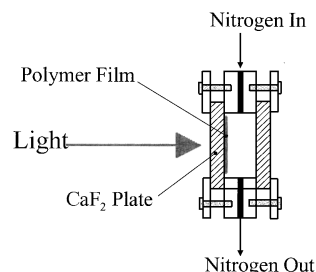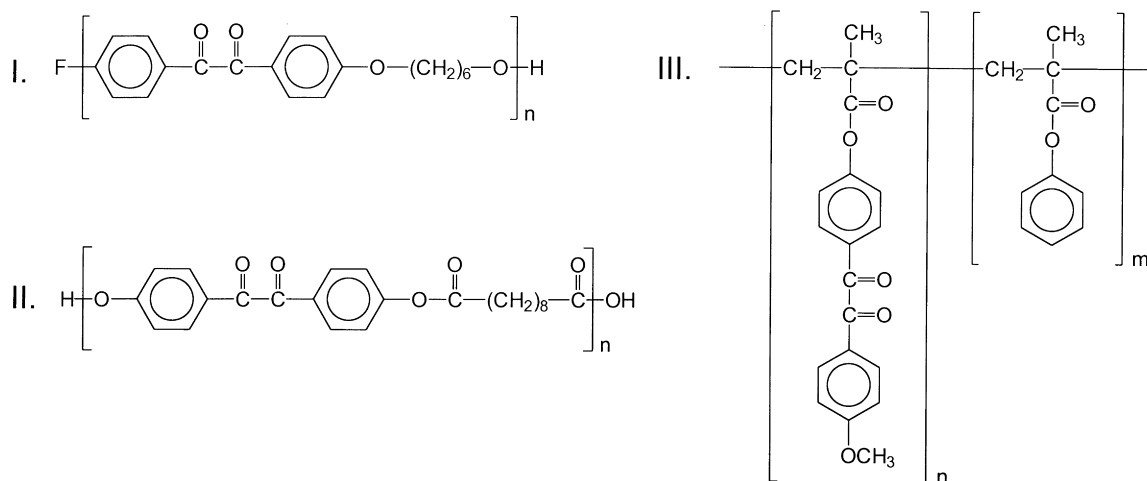

Fig. 2. Chamber for the u.v. irradiation of polymer films under inert gas.

Scheme 3.

gel 60), using cyclohexane/ethyl acetate (vol. ratio 10:8) as eluent 7.8 g (30 mmol, 40%) of 4-hydroxy-4′-methoxyben-zil were obtained. FT i.r. data (KBr pellet) are compiled in Table 1, ^{1}H n.m.r. data (acetone-d$_6$) are given in Table 2.

2.2.3. Synthesis of 4-methacryloyl-4′-methoxybenzil (MMB)

4-Hydroxy-4′-methoxybenzil (1.0 g, 3.9 mmol) was dissolved in a mixture of 2 cm^3 of dry methylene chloride and 3 cm^3 of pyridine. After cooling to 0°C, methacryloyl chloride (0.82 g, 7.8 mmol) was added dropwise. The mixture was stirred at room temperature for 2 h and poured into 11 cm^3 of water. Dichloromethane (4 cm^3) was added and then the solution was acidified with hydrochloric acid. The organic layer was separated and extracted with water (2 × 5 cm^3), a 10% aqueous solution of Na$_2$CO$_3$ (2 × 5 cm^3) and finally with water again (2 × 5 cm^3). The solution was dried over Na$_2$SO$_4$ and the solvent was evaporated in vacuo after filtration. The

oily residue was mixed with 0.4 cm^3 of methanol and allowed to crystallize at 4°C. After recrystallization from ethanol, 0.50 g (1.5 mmol) of 4-methacryloyl-4′-methoxybenzil were obtained (38%). For FT i.r. data (KBr pellet), see Table 1. For ^{1}H n.m.r. data (CDCl$_3$), see Table 2.

2.2.4. Synthesis of poly(oxyhexyleneoxy-4,4′-benzilylene) (polymer I) [21–23]

The polymer was prepared by polycondensation of 4,4′-difluorobenzil and 1,6-hexanediol. The reaction was carried out in phenyl sulfone in the presence of potassium carbonate (argon atmosphere). The mixture was heated for 60 min at 200°C and then for 120 min at 240°C. Care was taken to avoid sublimation of 4,4′-difluorobenzil. The crude reaction product was dissolved in dimethylformamide, filtered and precipitated from methanol. Further purification of the polymer was achieved by two-fold reprecipitation from dichloromethane/ethanol. Yield of polymer I: 18%. When 4,4′-dibromobenzil was employed instead of 4,4′-difluorobenzil, lower values for M_w were obtained.

^{1}H n.m.r data (CDCl$_3$) are collected in Table 2 and FT i.r. data are compiled in Table 3. The values for M_w, M_n and T_g are summarized in Table 4 and solubility properties in Table 5.

2.2.5. Synthesis of poly(oxy-4,4′-benzilyleneoxysebacoyl) (polymer II)

4,4′-Dihydroxybenzil (1.0 g, 4.12 mmol) was dissolved in a mixture of 2 cm^3 of acetone, 30 cm^3 of dichloromethane and 0.84 cm^3 of pyridine, subsequently 0.88 cm^3 (4.12 mmol) of sebacic acid chloride were added. After a reaction time of 60 s, the polycondensation mixture was poured into 300 cm^3 of ethanol. The crude polymer was purified by three-fold reprecipitation from methylene chloride/ethanol. Yield of polymer II: 73%.

^{1}H n.m.r data (CDCl$_3$) are collected in Table 2 and FT i.r. data are compiled in Table 3. The values for M_w, M_n and T_g are summarized in Table 4 and solubility properties in Table 5.

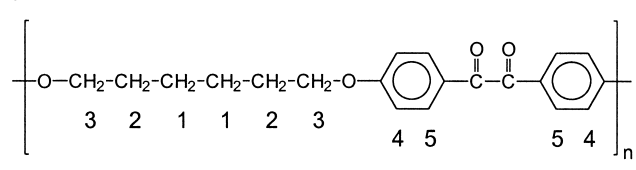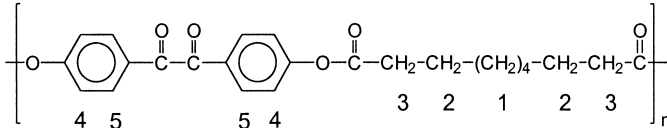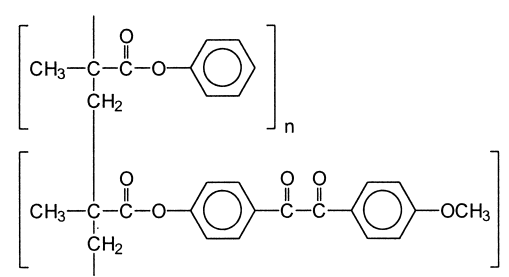Table 1
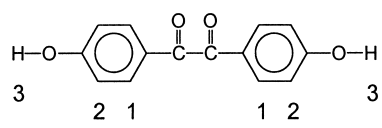FT i.r. data of low-molecular-weight compounds
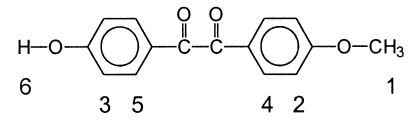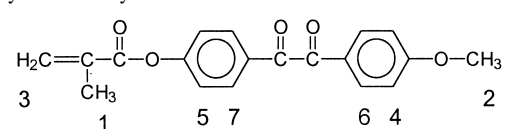
Wavenumber (in cm^{-1})			Assignment
MMB[a]	DHB[b]	HMB[c]	
	3400	3325	O–H stretch
2946		2920	C–H stretch
1739			C=O stretch (ester)
1669	1647	1660	C=O stretch (benzil units)
1597	1600	1597	C=C stretch (aromatic)
1507	1513	1511	C=C stretch (aromatic)
	1230	1267	C–O stretch, asym. (ether)
1214			C–O–C stretch (ester)
1160	1173	1160	C-phenyl stretch (keton)
		1022	C–O stretch, sym. (ether)
843			C–H bending (Aromatic, 1,4-disubstituted)
609	603	601	Benzil

[a] MMB = 4-methacryloyl-4′-methoxybenzil.
[b] DHB = 4,4′-dihydroxybenzil.
[c] HMB = 4-hydroxy-4′-methoxybenzil.

Table 2
[1]H n.m.r. data of low-molecular weight compounds and polymers I–III

Compound	Assignment	δ (ppm)	Coupling	Intensity
Polymer I	5	7.93	d	4H
−O−CH₂-CH₂-CH₂-CH₂-CH₂-CH₂-O− ...	4	6.96	d	4H
	3	4.03	t	4H
	2	1.82	m	4H
	1	1.55	m	4H
Polymer II	5	7.99	d	4H
−O− ... −O−C-CH₂-CH₂-(CH₂)₄-CH₂-CH₂-C−	4	7.21	d	4H
	3	2.53	t	4H
	2	1.73	m	4H
	1	1.36	m	8H
Polymer III	Aromatic	7.7–8.0		
	Aromatic	6.8–7.4		–
	−OCH₃	3.8	s	–
	−CH₃	2.3	s	–
	−CH₂−	1.5	s	–
4,4′-Dihydroxybenzil	3	9.74	s	2H
	2	7.83	d	4H
	1	6.97	d	4H
4-Hydroxy-4′-methoxybenzil	6	9.55	s	1H
	5	7.90	d	2H
	4	7.80	d	2H
	3	7.09	d	2H
	2	6.98	d	2H
	1	3.90	s	3H
4-Methacryloyl-4′-methoxybenzil	7	8.03	d	2H
	6	7.94	d	2H
	5	7.26	d	2H
	4	6.95	d	2H
	3b	6.35	s	1H
	3a	5.80	s	1H
	2	3.86	s	3H
	1	2.06	s	3H

2.2.6. Synthesis of poly(phenyl methacrylate-co-4-methacryloyloxy-4′-methoxybenzil) (polymer III)

To a solution of 4-methacryloyloxy-4′-methoxybenzil (0.10 g, 0.308 mmol) and phenyl methacrylate [24] (0.11 mg, 0.719 mmol) in 2.1 cm³ of dry tetrahydrofuran, 2.1 mg (0.013 mmol) of azoisobutyronitrile (AIBN) were added as free radical initiator. The reaction vessel was sealed under nitrogen and thermostated for 5 h at 60°C in

Table 3
FT i.r. data of polymers I–III

Wavenumber (in cm^{-1})			Assignment
Polymer I	Polymer II	Polymer III	
2937	2927	~2900	C–H stretch
2864	2855		C–H stretch
	1760	1750	C=O (ester)
1667	1672	1670	C=O (benzil units)
1593	1597	1596	C=C stretch (aromatic)
1503	1502	1488	C=C stretch (aromatic)
1240		1263	C–O stretch, asym. (ether)
	1210	1194	C–O–C stretch, asym. (ester)
1160	1160	1160	C-phenyl stretch (keton)
	1110	1102	C–O–C stretch, sym. (ester)
1014			C–O stretch, sym. (ether)
843	855	844	C–H bending (Aromatic, 1,4-disubstituted)
756	755		–
		745, 688	C–H bending (Aromatic, monosubstituted)

a water bath. The reaction was stopped by pouring the reaction mixture into 25 cm^3 of *n*-hexane. The crude copolymer was purified by two-fold reprecipitation from dichloromethane/methanol at −20°C. Yield of polymer III: 30%. Polymer III contained 30 mol-% of 4-methacryloyloxy-4′-methoxybenzil as calculated from ^{1}H n.m.r. spectra.

^{1}H n.m.r data (CDCl$_3$) are collected in Table 2 and FT i.r. data are compiled in Table 3. The values for M_w, M_n and T_g are summarized in Table 4 and solubility properties in Table 5.

3. Results and discussion

3.1. Irradiation of low-molecular-weight model compounds

To probe the photoreactivity of benzil, a solution of benzil in benzene (0.1 mol m^{-3}) was irradiated with the light of an excimer laser (308 nm, pulse energy 400 J m^{-2}). Even after irradiation energies up to 500 kJ m^{-2}, no reaction products, except traces of biphenyl, were detected by means of GC.

Following the procedure of McGimpsey and Scaiano [6],

an equimolar solution of benzil and 4,4′-dimethylbenzil in benzene (0.1 mol m^{-3} each) was irradiated with the excimer laser (308 nm). The appearance of the mixed coupling product 4-methylbenzil proved the homolytic fragmentation of benzil and 4,4′-dimethylbenzil as a result of a two-photon process. In our experiments, the pulse energy was varied between 30 and 700 J m^{-2}, but the total irradiation energy was 100 kJ m^{-2} in every case. The concentration of 4-methylbenzil in the irradiated solutions was determined by GC analysis. Fig. 3 shows the yield of 4-methylbenzil as a function of the laser pulse energy. At pulse energies between 30 and 300 J m^{-2}, the yield of 4-methylbenzil increased with the laser pulse energy. However, at higher pulse energies (range from 300 to 700 J m^{-2}), the yield of 4-methylbenzil remained essentially constant.

Our results derived from product analysis agree well with the spectral data reported by McGimpsey and Scaiano [6]. These researchers determined the formation of triplet benzil (T_1) at different pulse energies (40–200 J m^{-2}) by monitoring the optical density at 470 nm. For comparison, these data are inserted in Fig. 3 (dotted line).

In a control experiment, an equimolar solution of benzil and 4,4′-dimethylbenzil in benzene was irradiated with the Hg-lamp (313 nm, total energy 100 kJ m^{-2}). In this case, the formation of 4-methylbenzil was not observed.

3.2. FT i.r. measurements

It is reasonable to assume that in polymers I–III, the benzil units undergo photoreactions similar to those of low-molecular-weight model compounds in solution. Photoreactions of the diketo group should give rise to changes in the FT i.r. spectra of the polymers.

Fig. 4 shows FT i.r. spectra of a film of polymer I before and after laser irradiation. Regarding the spectrum of the unirradiated film, the band at 1667 cm^{-1} is assigned to the symmetric C=O stretch of the diketo group [25], while the strong signal at 1160 cm^{-1} is attributed to the phenyl-C stretch in aromatic ketones. The band at 1503 cm^{-1} and the doublet around 1600 cm^{-1} are due to vibrations of the aromatic ring. The ether units in polymer I give rise to bands at 1240 cm^{-1} (asymmetric C–O stretch) and 1014 cm^{-1} (symmetric C–O stretch) (compare Table 3).

After laser u.v. irradiation (pulse energy 400 J m^{-2}, total

Table 4
Characteristic data of polymers I–III

Polymer	M_n[a] (g mol^{-1})	M_w[a] (g mol^{-1})	$M_w \cdot M_n^{-1}$	Density (ρ)[b] (kg m^{-3})	T_g[c] (°C)	T_m (°C)	Degradation[d] (°C)
I	3700	8000	2.1	1220	71	–	> 350
II	12 000	24 000	2.0	1210	36	122	> 370
III	13 000	25 000	2.0	1250	–	–	> 290

[a] Rounded values; estimated error ≤10%.
[b] Determined by flotation in aqueous KI.
[c] Determined from DSC runs (midpoint).
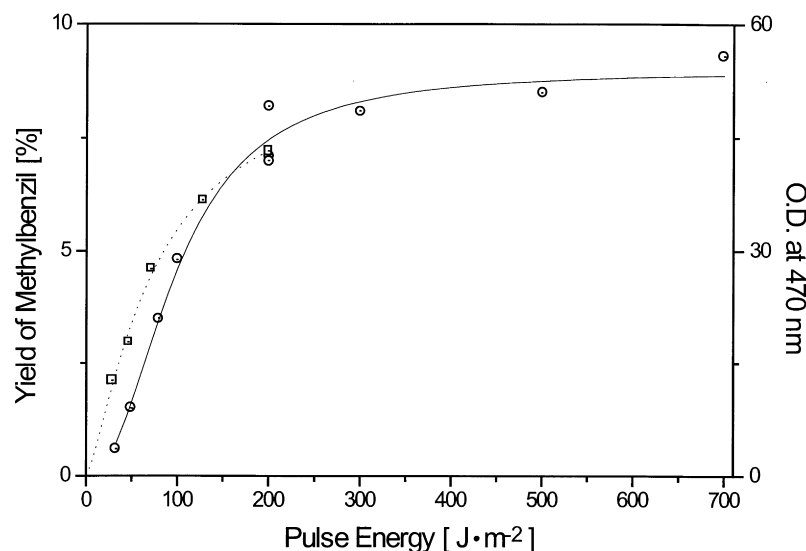[d] From thermogravimetric data (weight loss >5 wt.%).

Fig. 3. (○) Laser irradiation (308 nm) of a solution of benzil (0.1 mol m^{-3}) and 4,4$'$-dimethylbenzil (0.1 mol m^{-3}) in benzene. Yield of 4-methylbenzil as a function of the pulse energy at a constant total energy of 100 kJ m^{-2}. (□) Excitation of benzil with single 308 nm laser pulses: optical density at 470 nm (triplet benzil) 0.75 μs after the excitation as a function of the laser pulse energy (data taken from McGimpsey and Scaiano [6]).

energies 10 and 40 kJ m^{-2}), significant changes were observed in the FT i.r. spectrum (see Fig. 4). The intensity of the benzil C=O stretch at 1667 cm^{-1} and the signal at 1160 cm^{-1} decreased significantly. At the same time, a broad band in the range between 1700 and 1740 cm^{-1} evolved. The intensity of the aromatic ring vibration around 1600 cm^{-1} decreased and the doublet character of this band vanished. Generally, a doublet in the 1625–1575 cm^{-1} range is typical of aromatic rings bearing C=O (or C=C, C=N or NO$_2$) substituents directly conjugated to the ring [25], but a doublet is also observed with unsubstituted polystyrene. A reduction of the intensity (and also of the doublet character) of this band is another indication that the carbonyl group is transformed during u.v. irradiation. The photoreduction of benzil in hydrogen donating solvents to give benzoin is well known [2,5,9,26,27]. The FT i.r. spectrum of benzoin displays a C=O band around 1680 cm^{-1}. However, from the spectral changes in Fig. 4, the formation of benzoin units in polymer I could not be deduced. In addition, the formation of hydroxy groups (as would be characteristic of benzoin units) was not evidenced in the spectral range 3000–3400 cm^{-1}. Regarding the possibility of a homolytic cleavage of the benzil units in polymer I, one would expect the formation of aldehyde groups as a result of subsequent hydrogen abstraction. The i.r. absorption in the range 1700–1740 cm^{-1}, which was observed with polymer I after laser u.v. irradiation, may be attributed to aromatic aldehyde groups (aromatic aldehydes display an i.r. band with a maximum in the region between 1715 and 1685 cm^{-1}, see Ref. [25]). Additional signals in the range between 2745 and 2720 cm^{-1}, which would be typical of the C–H valence vibration of aldehydes [25], were not detectable in the FT i.r. spectrum. This may be due to the weak intensity of this band as is observed with several aromatic aldehydes (e.g. 4-ethoxybenzaldehyde and 4-(phenyloxy)benzaldehyde [28]).

Table 5
Solvents and non-solvents for polymers I–III

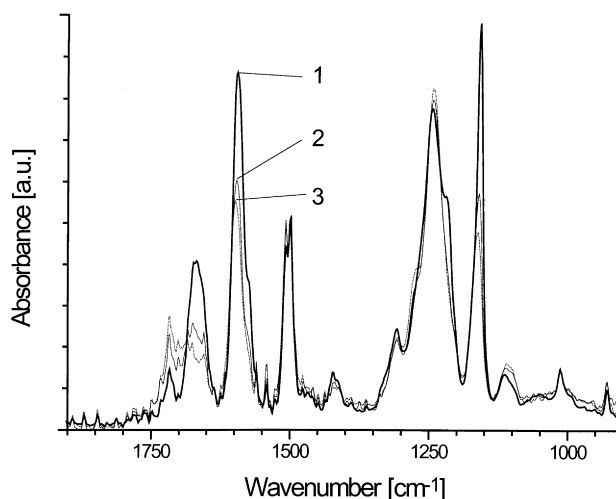| Polymer	Typical solvents	Typical non-solvents
I	Chloroform, methylene chloride, THF, DMF, acetone	Alcohols, alkanes
II	Chloroform, methylene chloride, pyridinium, THF,DMF, NMP	Alcohols, alkanes, benzene, acetone, acetonitrile
III	Chloroform, methylene chloride, acetone, pyridinium, THF, DMF, NMP	Alcohols, alkanes

Fig. 4. Changes in the FT i.r. absorbance spectrum of polymer I after irradiation with pulsed laser light (308 nm, pulse energy 400 J m^{-2}): (1) unirradiated polymer film; (2) irradiated with a total energy of 10 kJ m^{-2}; and (3) irradiated with a total energy of 40 kJ m^{-2}.
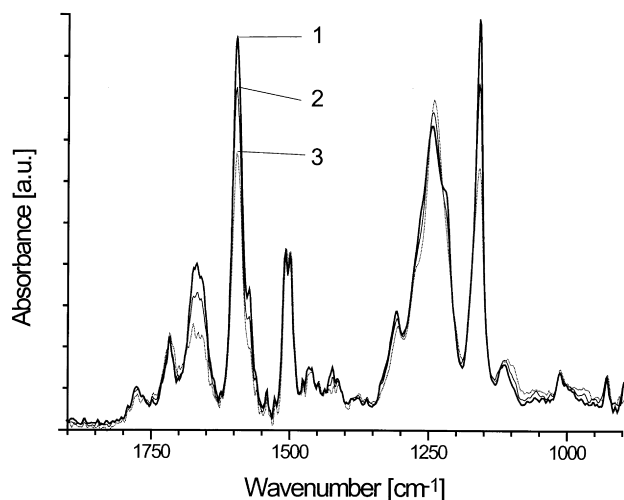
Fig. 5. Changes in the FT i.r. absorbance spectrum of polymer I when irradiated with a Hg-lamp (311 nm, intensity $18 \, J \, m^{-2} \, s^{-1}$): (1) unirradiated polymer film; (2) irradiated with a total energy of $10 \, kJ \, m^{-2}$; and (3) irradiated with a total energy of $40 \, kJ \, m^{-2}$.

Fig. 6. Changes in the FT i.r. absorbance spectrum of polymer II when irradiated with pulsed laser light (308 nm, pulse energy $400 \, J \, m^{-2}$): (1) unirradiated polymer film; (2) irradiated with a total energy of $10 \, kJ \, m^{-2}$; and (3) irradiated with a total energy of $40 \, kJ \, m^{-2}$.

The strong asymmetrical ether C–O stretching vibration at $1260 \, cm^{-1}$ and the weak symmetrical ether C–O stretching vibration at $1014 \, cm^{-1}$ remained essentially constant even after intense laser irradiation. Therefore, the ether units are not cleaved during u.v. irradiation and photo-Friess or photo-Claisen rearrangements do not proceed in polymer I. The intensity of the aromatic ring vibration at $1503 \, cm^{-1}$ did not change during laser irradiation. This indicates, first, that the aromatic rings in polymer I remain intact during laser u.v. irradiation and, second, that laser ablation does not occur.

In Fig. 5, FT i.r. spectra of polymer I before and after irradiation with the 311 nm line of a Hg-lamp are shown. The light intensity was $18 \, J \, m^{-2} \, s^{-1}$, the sample was irradiated with total energies between 10 and $40 \, kJ \, m^{-2}$, respectively. The benzil C=O stretch at $1667 \, cm^{-1}$ and the phenyl-C stretch at $1160 \, cm^{-1}$ decreased after irradiation, but no additional signals were observed in the carbonyl region. Again the intensity and the doublet character of the band around $1600 \, cm^{-1}$ decreased during irradiation, while the signal typical of the ether units remained almost unchanged. A comparison of the spectra in Figs. 4 and 5 shows that the photochemical conversion of the benzil units proceeds more effective under laser u.v. irradiation. This is most obvious in the early stage of the photoreaction (irradiation energy $10 \, kJ \, m^{-2}$). Summing up, both under laser and Hg-lamp irradiation the benzil units in polymer I are transformed. FT i.r. spectra indicate that both the reaction products and the efficiency of the photoreaction differ to some extent depending on the u.v. source. Although the photoproducts were not identified unambiguously from FT i.r. spectra, we suggest that a partial reduction of the benzil units and—under laser u.v. irradiation only—also a fission of the benzil units occur under u.v. irradiation.

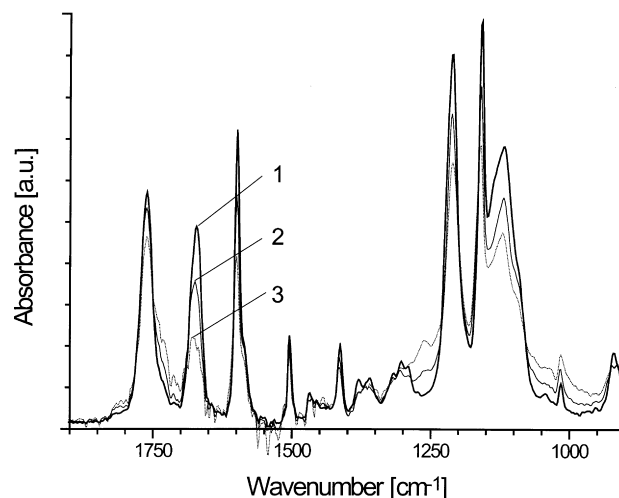The spectra given in Figs. 6 and 7 refer to polymer II

containing both benzil and ester groups. After laser u.v. irradiation, the intensity of the benzil C=O stretch ($1670 \, cm^{-1}$) decreased and additional absorption developed in the range between 1700 and $1740 \, cm^{-1}$ (see Fig. 6). Remarkably, the intensity of the ester C=O stretch ($1760 \, cm^{-1}$) also decreased by about 20% after an irradiation energy of $40 \, kJ \, m^{-2}$. At the same time, the signals typical of the asymmetrical and symmetrical ester C–O–C stretch (1210 and $1110 \, cm^{-1}$) lost in intensity. Regarding the band at $1600 \, cm^{-1}$ (aromatic ring vibration), changes similar to those in polymer I occurred.

Also under Hg-lamp irradiation of polymer II, the intensity of the benzil C=O band decreased (see Fig. 7). In this case, the decrease was far less than under excimer laser
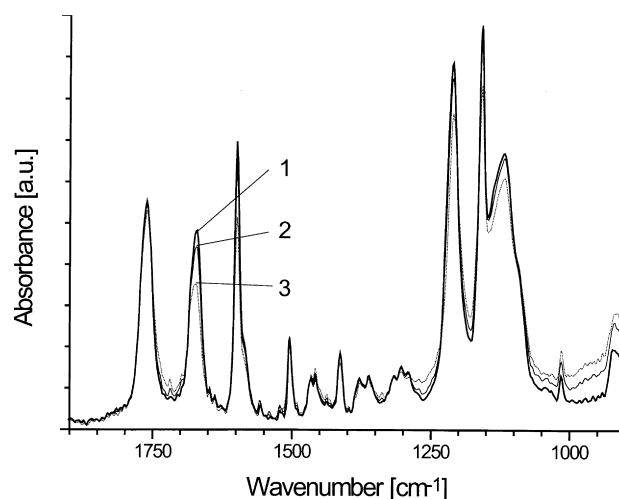

Fig. 7. Changes in the FT i.r. absorbance spectrum of polymer II when irradiated with a Hg-lamp (311 nm, light intensity $18 \, J \, m^{-2} \, s^{-1}$): (1) unirradiated polymer film; (2) irradiated with a total energy of $10 \, kJ \, m^{-2}$; and (3) irradiated with a total energy of $40 \, kJ \, m^{-2}$.
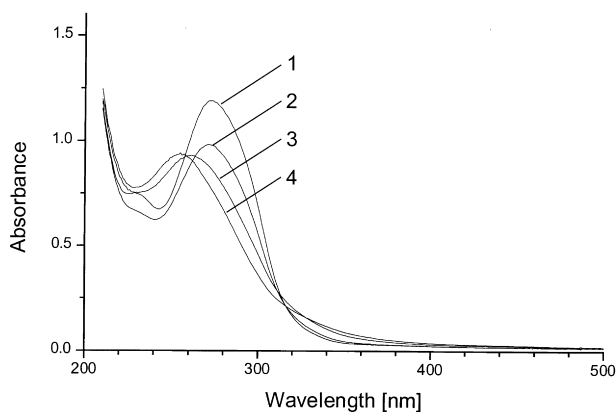
Fig. 8. U.v. spectra of polymer II (film on CaF$_2$ plate) after irradiation with an excimer laser (308 nm, pulse energy 100 J m^{-2}): (1) unirradiated film; (2) 10 kJ m^{-2}; (3) 50 kJ m^{-2}; and (4) 100 kJ m^{-2}.

radiation. Under Hg-lamp irradiation, the ester C=O band at 1760 cm^{-1} remained almost unchanged even after an irradiation energy of 40 kJ m^{-2}. At the same time, the intensity of the signals typical of the ester C–O–C stretch (1210 and 1110 cm^{-1}) decreased slightly, but the changes were far less than under laser u.v. irradiation. A significant conversion of the ester units was observed only after very intense illumination with the unfiltered light of the Hg-lamp. In this case, additional signals evolved at 1640 and 3380 cm^{-1}. While the band at 3380 cm^{-1} indicates the formation of OH groups, the signal at 1640 cm^{-1} is attributable to aromatic ketones bearing an OH group in the *ortho* position (for *o*-hydroxy diarylketones a band around 1645 cm^{-1} is reported [28]). The rearrangement of phenyl esters to give *ortho*-hydroxyketones is well known as the photo-*Friess* reaction, which proceeds via radical intermediates. In addition, a *Norrish*-type I fragmentation reaction of the ester units may also occur under u.v. irradiation [32].

The results obtained with polymer II show that the benzil units react both under excimer laser and under Hg-lamp irradiation. Similar to polymer I, the conversion of the benzil units proceeds with higher efficiency when the irradiation is carried out with the excimer laser. In the case of monochromatic u.v. irradiation (308 and 311 nm), a concomitant transformation of the ester groups was observed only under laser u.v. irradiation. Both the photo-*Friess* reaction as well as a *Norrish*-type I fragmentation may account for this finding.

When polymer III was irradiated, only small changes were observed in the FT i.r. spectra. This may be due to the fact that polymer III is a copolymer containing 70 mol-% of phenyl methacrylate units. These units exhibit low reactivity under u.v. irradiation.

3.3. U.v. measurements

The u.v. spectra of polymers I–III displayed pronounced changes upon u.v. irradiation. Because the changes were similar for all of these polymers, only the results obtained with polymer I will be discussed in detail.

Fig. 8 shows the u.v. spectra of polymer I before and after laser irradiation. The peak with a maximum at 273 nm is assigned to the Π–Π* transition of the benzil units. Laser u.v. irradiation caused a shift of the peak maximum towards lower wavelengths. After prolonged irradiation (100 kJ m^{-2}), the absorbance maximum was located at 255 nm. At the same time, the absorbance at the peak wavelength decreased significantly.

Monochromatic Hg-lamp irradiation (311 nm) lead to a similar result (see Fig. 9). However, the existence of isosbestic points at 258 and 322 nm indicates that the photoreaction proceeds uniformly. This was in contrast to the spectral changes after excimer laser irradiation.

It is appropriate to compare the u.v. spectra of polymer I with those of low-molecular-weight compounds. The Π–Π* transition of benzil (in methanol) has its maximum at $\lambda_{max} = 259$ nm ($\varepsilon_{max} = 2080$ m^2 mol^{-1}), whereas benzoin (in methanol) displays an absorption maximum at $\lambda_{max} = 246$ nm ($\varepsilon_{max} = 1240$ m^2 mol^{-1}). Benzaldehyde absorbs at $\lambda_{max} = 244$ nm with $\varepsilon_{max} = 610$ m^2 mol^{-1}. The spectral changes observed in films of polymer I (Figs. 8 and 9) support the view that the benzil units are transformed during irradiation. However, the nature of the photoproducts cannot be deduced from u.v. data. In particular, the absorption maxima of benzoin and benzaldehyde are too close to each other to allow differentiation.

In microlithography, it is desirable that photoresist materials show a depletion of absorbance at the irradiation wavelength. This "photobleaching" effect [29] enables light to penetrate the whole thickness of the resist film. Photobleaching is also seen with our polymers I–III in the spectral range 260–320 nm.

3.4. Quantitative evaluation of crosslinking data

For the characterization of resist materials, exposure curves are commonly used. Here the normalized film thickness (between 0 and 1.0) is plotted as a function of the irradiation energy E' (in J m^{-2}). The irradiation energy E'_g (in J m^{-2}), where gelation begins, as well as the contrast behaviour of the resist material are readily determined.

The quantum efficiency of photocrosslinking (Φ_{CL}) and chain scission (Φ_{CS}) in polymers can be derived from sol–gel data by applying the Charlesby–Pinner relationship [30]. This formalism has been derived for linear polymers with a most probable molecular weight distribution ($M_w \cdot M_n^{-1} = 2$). Crosslinking and chain scission are presumed to occur at random and independent of the molecular weight and the degree of crosslinking. Considering the polydispersity of the polymers I–III ($2.0 < M_w \cdot M_n^{-1} < 2.1$), the Charlesby–Pinner relationship can be regarded as a useful approximation in these cases. We processed the crosslinking data
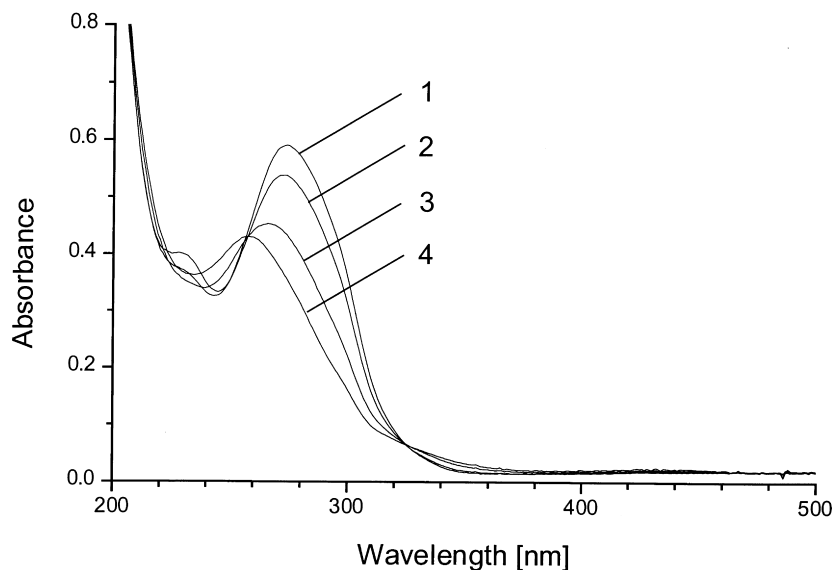
Fig. 9. U.v. spectra of polymer II (film on CaF$_2$ plate) after irradiation with the continuous light of a Hg-lamp (313 nm, intensity 18 J m^{-2} s^{-1}): (1) unirradiated film; (2) 10 kJ m^{-2}; (3) 50 kJ m^{-2}; and (4) 100 kJ m^{-2}.

according to Eq. (1) [31]:

$$S + \sqrt{S} = \alpha \frac{1}{\gamma} + 2E_g^0 \frac{1}{E} \tag{1}$$

where S is the soluble fraction of the polymer, α the number of chain scissions per unit of radiation dose and γ the number of monomer units crosslinked per unit of radiation dose. E is the energy of radiation (dose) absorbed in the polymer film (in mole photons per kg of polymer) and E_g^0 a virtual gel dose that would be observed in the absence of chain scission (E_g^0 in mole photons per kg of polymer). If the Charlesby–Pinner relationship is valid for a given polymer, a plot of $S + \sqrt{S}$ versus E^{-1} gives a straight line. Extrapolation to $S + \sqrt{S} = 2$ (onset of gel formation) gives the actual gel dose E_g, extrapolation to $S + \sqrt{S} = 0$ gives the ratio $\alpha \gamma^{-1}$. Φ_{CL} is then derived from the following equation (compare Ref. [32]):

$$\Phi_{CL} = \frac{1}{M_w E_g^0} \tag{2}$$

The net quantum efficiency of crosslinking ($\Phi_{CL,CS}$), which describes the overall process, was calculated from:

$$\Phi_{CL,CS} = \frac{1}{M_w E_g} \tag{3}$$

where E_g is the actual gel dose. Finally, Φ_{CS} was obtained

from Ref. [30]:

$$\frac{\alpha}{\gamma} = \frac{\Phi_{CS}}{\Phi_{CL}} \tag{4}$$

3.5. Photocrosslinking and chain scission in polymers I–III

The polymers I–III became crosslinked upon u.v. irradiation. Generally, crosslinking in these polymers may be due to photoreactions of the benzil units (compare Scheme 2). As an example, a possible reaction sequence involving radical intermediates is depicted in Scheme 4 (proposed reaction scheme for the formation of crosslinks in polymers I and II via ketyl radicals). The recombination of main chain radicals then leads to the formation of crosslinks. As discussed above, other photoreactions involving the benzil units also seem to occur. In the case of polymer II, the fission of the main-chain ester units (photo-*Friess* and *Norrish*-type I reaction) is expected to contribute to chain fragmentation. Similar reactions may occur in polymer III, which contains pendant phenyl ester units.

Table 6 summarizes the data on E'_g, E_g, E°_g, Φ_{CL}, $\Phi_{CL,CS}$ and Φ_{CS} as derived from Eqs. (1)–(4). Fig. 10 displays the sol–gel curves obtained from polymer I. Under high-intensity laser irradiation (pulse energy 400 J m^{-2}), the onset of gel formation occurred at $E'_g \sim 260$ J m^{-2}. Laser irradiation with
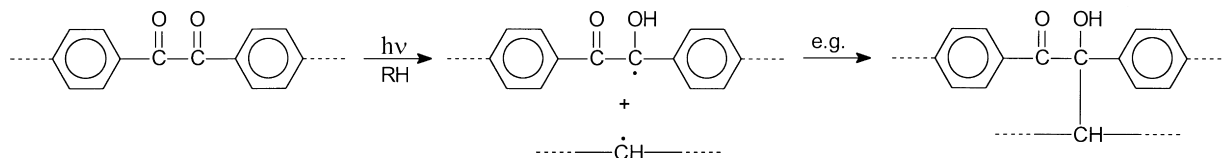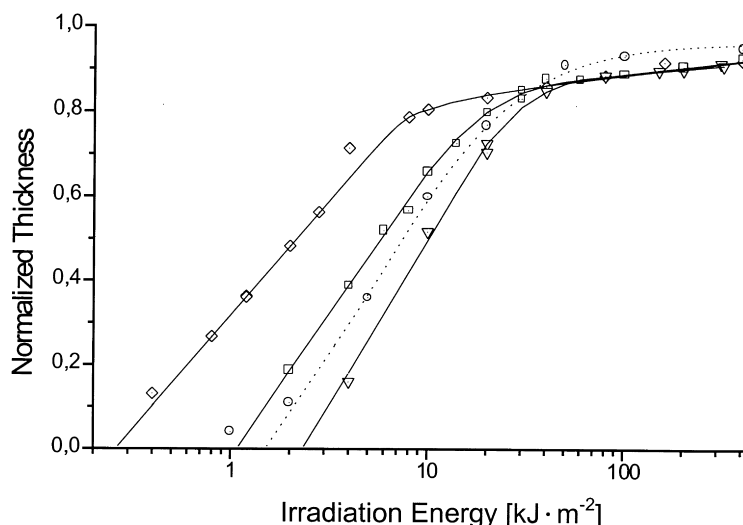

Scheme 4.

Fig. 10. Photocrosslinking of polymer I under different irradiation conditions: normalized film thickness as a function of irradiation energy. ($\bigcirc$) Hg-lamp (311 nm, intensity 18 J m^{-2} s^{-1}), ($\triangledown$) laser, 308 nm, pulse energy 100 J m^{-2}; ($\square$) laser, 308 nm, pulse energy 200 J m^{-2}; ($\diamond$) laser, 308 nm, pulse energy 400 J m^{-2}.

lower pulse energies (100 and 200 J m^{-2}, respectively) yielded $E'_g \sim 2300$ and $E'_g \sim 1100$ J m^{-2}. Under continuous Hg-lamp irradiation, a value of $E'_g \sim 1500$ J m^{-2} was obtained.

Fig. 11 contains the corresponding plots of $S + \sqrt{S}$ versus E^{-1}. The Charlesby–Pinner analysis of the sol–gel data (see Table 6) showed that both crosslinking and chain fragmentation occur during irradiation. The ratio $\Phi_{CS} \cdot \Phi_{CL}^{-1}$ remained similar under all irradiation conditions ($0.24 < \Phi_{CS} \cdot \Phi_{CL}^{-1} < 0.36$). At the same time, both the quantum efficiencies of crosslinking and chain scission increased as the pulse energy of the laser was raised. At a pulse energy of 100 J m^{-2}, we obtained $\Phi_{CL} \sim 7 \times 10^{-3}$ and $\Phi_{CS} \sim 2 \times 10^{-3}$. Comparable values were found under Hg-lamp irradiation. However, laser irradiation with a pulse energy of 400 J m^{-2} gave $\Phi_{CL} \sim 48 \times 10^{-3}$ and $\Phi_{CS} \sim 17 \times 10^{-3}$.

The results show that the overall reactivity of polymer I increased as the pulse energy of the excimer laser was raised. Compared to continuous Hg-lamp irradiation, the lithographic sensitivity of polymer I was enhanced by a

factor of five when intense excimer laser radiation was applied.

Similar results were obtained with polymer II (see the sol–gel curves in Fig. 12). Under high-intensity laser irradiation (pulse energy 400 J m^{-2}), the onset of gel formation occured at $E'_g \sim 1400$ J m^{-2}, with lower pulse energies (100 J m^{-2}) the onset of gel formation was observed around $E'_g = 3500$ J m^{-2}. The Charlesby–Pinner plots are shown in Fig. 13 and the corresponding data are given in Table 6. The quantum efficiencies Φ_{CL} of crosslinking were comparable, when the irradiation was carried out with the Hg-lamp or with laser pulses of 100 J m^{-2} ($\Phi_{CL} \sim 2.5 \times 10^{-3}$ and $\Phi_{CL} \sim 1.8 \times 10^{-3}$, respectively). With a pulse energy of 400 J m^{-2}, we obtained $\Phi_{CL} \sim 8.9 \times 10^{-3}$. At the same time, the efficiency of chain scissioning was raised from $\Phi_{CS} \sim 1.1 \times 10^{-3}$ (Hg-lamp) to $\Phi_{CS} \sim 4.8 \times 10^{-3}$ (pulse energy 400 J m^{-2}). Again the ratio $\Phi_{CS} \cdot \Phi_{CL}^{-1}$ remained similar under all irradiation conditions ($0.44 < \Phi_{CS} \cdot \Phi_{CL}^{-1} < 0.54$).

Similar to polymer I, the overall reactivity of polymer II increased significantly when the irradiation was carried out

Table 6
Quantitative data on photoinduced crosslinking and chain fragmentation in polymers I–III

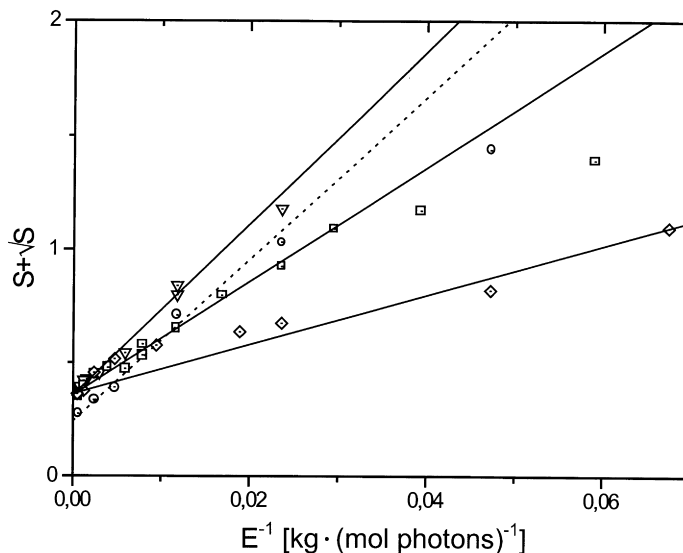| Polymer	Irradiation	E'_g (J m^{-2})	E_g (mole photons kg^{-1})	$E°_g$ (mole photons kg^{-1})	$\Phi_{CL,CS}$	Φ_{CL}	Φ_{CS}	$\Phi_{CS} \cdot \Phi_{CL}^{-1}$
I	Hg-lamp	1500	17	15	7.3×10^{-3}	8.3×10^{-3}	2.0×10^{-3}	0.24
	Laser 100 J m^{-2}	2300	23	19	5.4×10^{-3}	6.6×10^{-3}	2.4×10^{-3}	0.36
	Laser 400 J m^{-2}	260	4	3	36×10^{-3}	48×10^{-3}	17×10^{-3}	0.35
II	Hg-lamp	~2700	19	17	2.2×10^{-3}	2.5×10^{-3}	1.1×10^{-3}	0.44
	Laser 100 J m^{-2}	3500	31	23	1.3×10^{-3}	1.8×10^{-3}	1.0×10^{-3}	0.54
	Laser 400 J m^{-2}	1400	6	5	6.6×10^{-3}	8.9×10^{-3}	4.8×10^{-3}	0.54
III	Hg-lamp	1700	17	–	3×10^{-3}	–	–	–
	Laser 50 J m^{-2}	2000	21	–	2×10^{-3}	–	–	–
	Laser 330 J m^{-2}	300	3	–	10×10^{-3}	–	–	–

Fig. 11. Photocrosslinking of polymer I under different irradiation conditions: Charlesby–Pinner evaluation of the crosslinking data. (○) Hg-lamp, 311 nm, intensity 18 J m^{-2} s^{-1}; (▽) laser, 308 nm, pulse energy 100 J m^{-2}; (□) laser, 308 nm, pulse energy 200 J m^{-2}; (◇) laser, 308 nm, pulse energy 400 J m^{-2}.

with laser pulses of high energy (400 J m^{-2}). Compared to the results obtained with the Hg-lamp or with lower pulse energy, both Φ_{CL} and Φ_{CS} were raised by a factor of five. This resulted in an enhancement of the lithographic sensitivity by a factor of three to four. A comparison of the photoreactivities of polymers I and II shows that photocrosslinking in polymer I proceeds with higher quantum efficiency Φ_{CL} than in polymer II. If the crosslinking reaction proceeds via hydrogen abstraction (as suggested in Scheme 4), a lower reactivity would be predicted for polymer I as it contains less labile hydrogen atoms per repeating unit than polymer II. Differences in the mobility of the polymer chains and in the balance of intermolecular and intramolecular crosslinking may account for this contradictory result.

Polymer III became fully crosslinked (100%) under low-intensity laser irradiation (pulse energy 50 J m^{-2}) and under Hg-lamp irradiation. The onset of gel formation was observed at similar E'_g values ($E'_g \sim 2000$ J m^{-2} under low-intensity laser irradiation and $E'_g \sim 1700$ J m^{-2} under Hg-lamp irradiation). Employing high-intensity laser radiation (pulse energy 330 J m^{-2}), the gel dose dropped to $E'_g \sim 300$ J m^{-2} (see Fig. 14). This demonstrates an enhancement of the lithographic sensitivity by a factor between six and seven. Upon prolonged irradiation with a pulse energy of 330 J m^{-2}, the sensitivity curve reached a maximum near $E' = 10^4$ J m^{-2}. At irradiation energies $E' > 10^4$ J m^{-2}, the solubility increased, which indicates a degradation of the polymer. A Charlesby–Pinner evaluation of the crosslinking
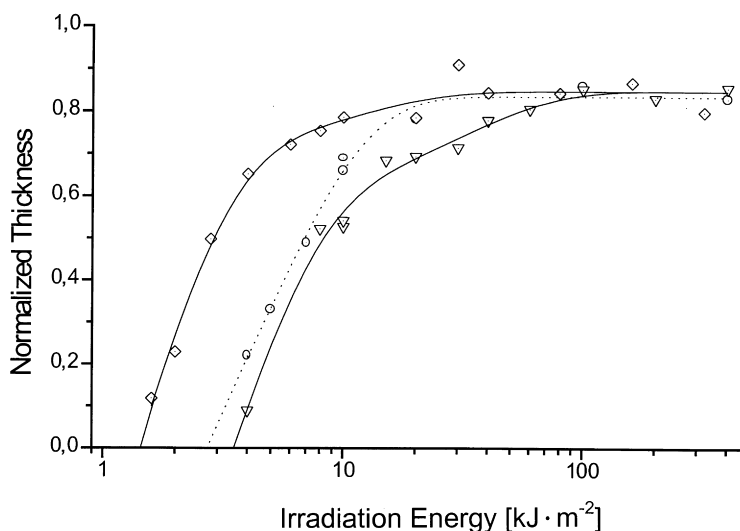

Fig. 12. Photocrosslinking of polymer II under different irradiation conditions: normalized film thickness as a function of irradiation energy. (○) Hg-lamp, 311 nm, intensity 18 J m^{-2} s^{-1}; (▽) laser, 308 nm, pulse energy 100 J m^{-2}; (◇) laser, 308 nm, pulse energy 400 J m^{-2}.
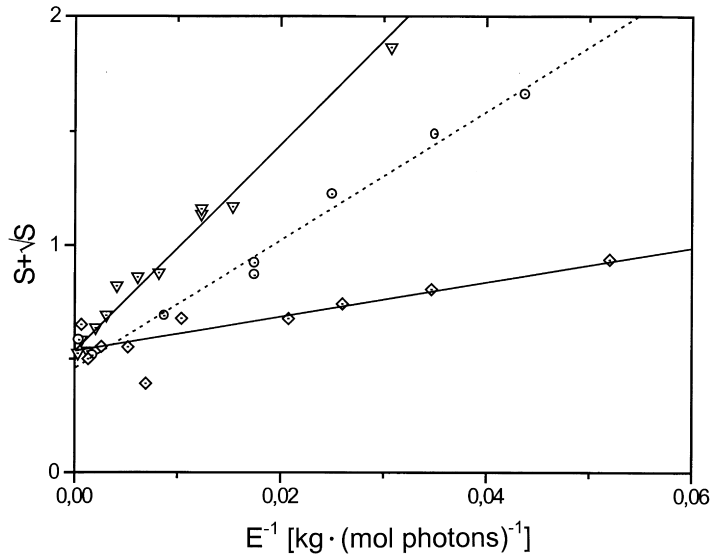
Fig. 13. Photocrosslinking of polymer II under different irradiation conditions: Charlesby–Pinner evaluation of the crosslinking data. (○) Hg-lamp, 311 nm, intensity 18 J m^{-2} s^{-1}; (▽) laser, 308 nm, pulse energy 100 J m^{-2}; (◇) laser, 308 nm, pulse energy 400 J m^{-2}.

data was not appropriate in the case of polymer III, since straight line fits were not obtained. Therefore, we employed the following equation to determine the overall quantum yield $\Phi_{CL,CS}$ from the gel dose E'_g (compare Ref. [32]):

$$\Phi_{CL,CS} = \frac{rd}{AM_w E'_g} \tag{5}$$

Under Hg-lamp irradiation $\Phi_{CL,CS}$ was 3×10^{-3}. Employing low-intensity laser pulses (50 J m^{-2}), a similar value $\Phi_{CL,CS} = 2 \times 10^{-3}$ was obtained. High-intensity laser irradiation raised $\Phi_{CL,CS}$ to 10×10^{-3}. The final degradation of polymer III under intense laser u.v. light may proceed in a similar way as has been reported for polymethyl methacrylate [32]: Norrish-type I fragmentation of

the pendant ester units and subsequent scission of the main chain. Obviously, this degradation does not take place under Hg-lamp and low-energy laser radiation.

3.6. Possibility of thermal reactions

When materials are irradiated with a laser light source, thermal reactions may also occur. To estimate the heating of the polymer films under investigation, we used the following equation:

$$dT = \frac{dQ_m}{c_p} \tag{6}$$

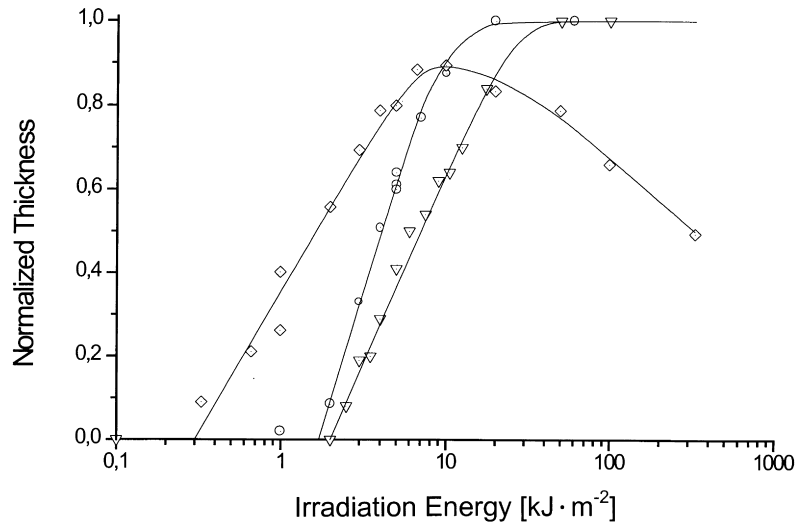where c_p denotes the specific heat capacity. For most

Fig. 14. Photocrosslinking of polymer III under different irradiation conditions: normalized film thickness as a function of irradiation energy. (○) Hg-lamp, 311 nm, intensity 18 J m^{-2} s^{-1}; (▽) laser, 308 nm, pulse energy 50 J m^{-2}; (◇) laser, 308 nm, pulse energy 330 J m^{-2}.

polymers, c_p values (25°C) range between 1000 and 2000 J kg^{-1} K^{-1} (Ref. [33]).

Films of polymers I and II, having a thickness of 0.25 μm, absorb a light fraction of approximately 0.36 at the irradiation wavelength (308 nm). Assuming an average heat capacity $c_p = 1.5$ kJ kg^{-1} K^{-1} and a density $\rho = 1220$ kg m^{-3}, we obtain the following ΔT values for 0.25 μm films, when heat transfer to the substrate during the duration of a laser pulse (20 ns) is neglected: $\Delta T = 80$°C at low-intensity laser irradiation with a single pulse of 100 J m^{-2}, $\Delta T = 315$°C at high-intensity laser irradiation with a single pulse of 400 J m^{-2}.

These values indicate that laser irradiation causes thermal heating of the polymer films. Thermogravimetric and DSC data showed that polymers I and II are thermally stable up to approximately 350°C, while polymer III begins to degrade at temperatures above 290°C (Table 1). Consequently, we conclude that thermal degradation is not important for polymers I–III during laser irradiation. This is consistent with the fact that laser ablation was not observed in our experiments. Although thermal effects cannot be entirely neglected, the variation of the photosensitivity of the polymers with the laser pulse energy may be a result of two-photon processes.

4. Conclusions

Polymers containing benzil units in the main chain (polymers I and II) or as pendant groups (polymer III) can be applied as negative toned photoresist materials.

We were able to show that the lithographic sensitivity of these materials depended upon the irradiation source (Hg-lamp, 311 nm; excimer laser, 308 nm) and the pulse energy of the excimer laser. When the pulse energy of the laser was raised, an increase of the lithographic sensitivity by a factor of up to 4–6 was observed. This means that the lithographic sensitivity of these polymers can be "tuned" by adjusting the laser pulse energy.

A Charlesby–Pinner analysis of crosslinking data revealed that both the quantum efficiency of crosslinking (Φ_{CL} and $\Phi_{CL,CS}$) and the quantum efficiency of chain scission (Φ_{CS}) increased as the laser energy was raised.

FT i.r. and u.v. spectroscopy showed that the benzil units in polymers I and II are depleted during u.v. irradiation (both under the Hg-lamp and under the laser u.v. light). As concluded from FT i.r. data, the transformation of the benzil units occurs with higher efficiency (and also with other reaction products) when intense laser u.v. light is employed. Under such irradiation conditions, additional photoreactions occur in the polymers. For example, the degradation of the ester units in polymer II is considerable under intense laser light (308 nm), but remains minor under monochromatic Hg-lamp irradiation with 311 nm.

Such laser-specific reactions, which are probably due to two-photon effects, give rise to variations of the lithographic sensitivity with the laser pulse energy. Until today, two-photon effects have been reported for only a limited number of organic compounds (benzil, dinaphthyl propanones [7], stilbene derivatives [34] and benzyl esters [35]). It appears promising to investigate the lithographic behaviour of polymers bearing such organic groups. Investigations on polymers containing benzyl ester units are currently in progress.

Acknowledgements

References

[1] Rabek JF. Mechanisms of photophysical processes and photochemical reactions in polymers. Chichester: Wiley, 1987.
[2] Bunbury DL, Chan TM. Can J Chem 1972;50:2499.
[3] Ledwith A, Russel PJ, Sutcliffe LH. J Chem Soc, Perkin Trans 1972;2:1925.
[4] Encinas MV, Scaiano JC. J Am Chem Soc 1979;101:7740.
[5] Das Mohapatra GK, Bhattacharya J, Bandopadhyay J, Bera SC. J Photochem Photobiol A 1987;40:47.
[6] McGimpsey WG, Scaiano JC. J Am Chem Soc 1987;109:2179.
[7] Scaiano JC, Johnston LJ, McGimpsey WG, Weir D. Acc Chem Res 1988;21:22.
[8] Mukai M, Yamauchi S, Hirota N. J Phys Chem 1989;93:4411.
[9] Mukai M, Yamauchi S, Hirota N. J Phys Chem 1992;96:3305.
[10] Fischer H, Baer R, Hany R, Verhoolen I, Walbiner M. J Chem Soc, Perkin Trans 1990;2:787.
[11] Adam W, Oestrich RS. J. Am Chem Soc 1993;115:3455.
[12] Lukác I, Kósa C. Macromol Rapid Commun 1994;15:929.
[13] Kósa C, Lukác I. Chem Listy 1996;90:287.
[14] Hutchinson J, Ledwith A. Polymer 1973;14:405.
[15] Hilborn J, Ranby B. Macromolecules 1989;22:1154.
[16] Lukác I, Zvara I, Hrdlovic P. Eur Polym J 1982;18:427.
[17] Lukác I, Hrdlovic P. Macromol Chem Phys 1994;195:2233.
[18] Thompson LF, Willson CG, Bowden MJ, editors. Introduction to microlithography Washington, DC: American Chemical Society, 1994.
[19] Bendig J, Mitzner R, Dähne L. Macromol Chem Phys, Macromol Symp 1988;18:145.
[20] Hatchard CG, Parker CA. Proc R Soc London, Ser A 1956;235:518.
[21] Brandukova NE, Vygodski YS, Vinogradova SV, Raubach H. Acta Polym 1991;42:82.
[22] Strukelj M, Hedrick JC. Macromolecules 1994;27:7511.
[23] Strukelj M, Hedrick JC, Hedrick JL, Twieg RJ. Macromolecules 1994;27:6277.
[24] Ayrey G, Haynes AC. Eur Polym J 1973;9:1029.
[25] Socrates G. Infrared characteristic group frequencies. Chichester: Wiley, 1994.
[26] Blätter C, Paul H. Res Chem Intermed 1991;16:201.
[27] Mukherjee J, Sen D, Bera SC. Proc Indian Acad Sci, Chem Sci 1992;104:693.
[28] Pouchert CJ. The Aldrich library of infrared spectra. III ed.. Milwaukee, WI: Aldrich Chemical Company Inc, 1981.
[29] Willson CG, Bowden MJ. In: Bowden MJ, Turner SR, editors.

Electronic and photonic applications of polymers, Advances in chemistry series 218 Washington, DC: American Chemical Society, 1989.

[30] Charlesby A, Pinner SH. Proc R Soc London, Ser A 1959;249:367.

[31] David C, Borsu M, Geuskens G. Eur Polym J 1970;6:959.

[32] Reiser A. Photoreactive polymers. New York: Wiley, 1989.

[33] Brandrup J, Immergut EH, editors. Polymer handbook New York: Wiley, 1975.

[34] Cumpston BH, et al. Nature 1999;398:51.

[35] Shepelin EB, Bagdasaryan KS. Khim Vys Energ 1989;23:67 (Chem Abstr 110: 144709a).